

LOCAL PERCEPTION AND LEARNING MECHANISMS IN RESOURCE-CONSUMER DYNAMICS*

QINGYAN SHI[†], YONGLI SONG[‡], AND HAO WANG[§]

Abstract. Spatial memory is key in animal movement modeling, but it has been challenging to explicitly model learning to describe memory acquisition. In this paper, we study novel cognitive consumer-resource models with different consumer learning mechanisms and investigate their dynamics. These models consist of two PDEs in composition with one ODE such that the spectrum of the corresponding linearized operator at a constant steady state is unclear. We describe the spectra of the linearized operators and analyze the eigenvalue problems to determine the stability of the constant steady states. We then perform bifurcation analysis by taking the perceptual diffusion rate as the bifurcation parameter. It is found that steady-state and Hopf bifurcations can both occur in these systems, and the bifurcation points are given so that the stability region can be determined. Moreover, rich spatial and spatiotemporal patterns can be generated in such systems via different types of bifurcation. Our effort establishes a new approach to tackling a hybrid model of PDE-ODE composition and provides a deeper understanding of cognitive movement-driven consumer-resource dynamics.

Key words. perceptual diffusion, resource-consumer, PDE-ODE model, pattern formation, Hopf bifurcation, steady-state bifurcation

MSC codes. 34K18, 92B05, 35B32, 35K57

DOI. 10.1137/23M1598593

1. Introduction. Since 1952, Turing instability [38] induced by random diffusion has been highly esteemed as the mechanism for the spatial heterogeneous distribution of species in nature. However, numerous pieces of evidence show that random diffusion is insufficient to describe the animal movement as many factors may affect the animals' decision for spatial movement. Some clever animals even exhibit amazing cognition in choosing their favored habitat. Therefore, the cognition of animals should be taken into consideration in animal movement modeling [6, 9, 19]. Although specific mechanisms are still in debate, most modelers believe that perception (information acquisition) and memory (the retention of information) play dominant roles in interpreting complicated animal movement behaviors. Generally speaking, perception is the process by which animals acquire information, while memory is the

*Received by the editors September 5, 2023; accepted for publication (in revised form) March 5, 2024; published electronically May 13, 2024.

<https://doi.org/10.1137/23M1598593>

Funding: The first author was partially supported by the National Natural Science Foundation of China (12001240, 12271216) and the Natural Science Foundation of Jiangsu Province (BK20200589). The second author was supported by the National Natural Science Foundation of China (12371166) and the Zhejiang Provincial Natural Science Foundation of China (LZ23A010001). The third author was partially supported by the Natural Sciences and Engineering Research Council of Canada (Individual Discovery grant RGPIN-2020-03911 and Discovery Accelerator Supplement award RGPAS-2020-00090) and the Canada Research Chairs program (Tier 1 Canada Research Chair Award).

[†]School of Science, Jiangnan University, Wuxi, Jiangsu, 214122, China (qingyanshi@jiangnan.edu.cn).

[‡]School of Mathematics, Hangzhou Normal University, Hangzhou, Zhejiang, 311121, China (songyl@hznu.edu.cn).

[§]Corresponding author. Department of Mathematical and Statistical Sciences, University of Alberta, Edmonton, AB T6G 2G1, Canada (hao8@ualberta.ca).

storage, encoding, and recalling of information. Spatial memory is the memory of spatial locations in a living organism’s landscape. A strong motivation for the significance of spatial memory in animal movements is the empirical evidence of blue whale migrations presented by [1] and discussed by [4]. Much progress has been made in incorporating spatial cognition or memory implicitly, such as home range analysis [17, 18], scent marks [12], taxis-driven pattern formation [21, 22], information gaining through the last visit to locations [23], perceptual ranges [5], and delayed resource-driven movement [8].

In [5], Fagan et al. proposed a resource-driven movement model for studying perceptual ranges and foraging success, and the delay effect was later considered in the resource-driven movement model in [8]. In [41], by assuming that the consumers have knowledge of where the resources are, Wang and Salmaniw proposed the following consumer-resource model with an additional term biasing the movement of the consumer:

$$(1.1) \quad \begin{cases} u_t = d_1 \Delta u + u \left(1 - \frac{u}{k}\right) - \frac{muv}{1+u}, & x \in \Omega, t > 0, \\ v_t = d_2 \Delta v - \chi \nabla \cdot (v \nabla \bar{q}) + \frac{muv}{1+u} - dv, & x \in \Omega, t > 0, \\ \partial_\nu u = \partial_\nu v = 0, & x \in \partial\Omega, t > 0, \end{cases}$$

where $u = u(x, t)$ and $v = v(x, t)$ denote the density of resource and consumer, respectively. In the model, it is assumed that the perceptual ability of the consumer may not be uniform across varying distances, which can be reflected by a nonlocal perception. The perceptual function $\bar{q}(x, t)$ incorporating both distance and quality of detection is of the form

$$\bar{q}(x, t) = \int_{\Omega} g_R(x - y)q(y, t)dy,$$

where $g_R(x - y)$ is the perceptual kernel and depends on the perceptual range R . For the biological meaning, $g_R(x)$ should satisfy the following hypotheses [41]:

- (i) $g_R(x)$ is symmetric about the origin and nonincreasing from the origin;
- (ii) $\int_{\Omega} g_R(x)dx = 1$, and $\lim_{R \rightarrow 0^+} g_R(x) = \delta(x)$.

A typical example that satisfies the above two hypotheses is the so-called top-hat function:

$$g_R(x) = \begin{cases} \frac{1}{2R}, & -R < x < R, \\ 0 & \text{otherwise.} \end{cases}$$

Recently, there has been increasing interest and effort in studying the influence of the perceptual range on population dynamics [33, 41, 45].

In this paper, we explore the limiting scenario when the perceptual range approaches zero, i.e., $R \rightarrow 0^+$. For this local perception scenario, $g_R(x) = \delta(x)$ and system (1.1) becomes

$$(1.2) \quad \begin{cases} u_t = d_1 \Delta u + u \left(1 - \frac{u}{k}\right) - \frac{muv}{1+u}, & x \in \Omega, t > 0, \\ v_t = d_2 \Delta v - \chi \nabla \cdot (v \nabla q) + \frac{muv}{1+u} - dv, & x \in \Omega, t > 0, \\ \partial_\nu u = \partial_\nu v = 0, & x \in \partial\Omega, t > 0. \end{cases}$$

The parameters in (1.2) are all positive constants except for $\chi \in \mathbb{R}$: d_1, d_2 denote the random diffusion rates for resource and consumer, respectively; k is the carrying

capacity for resource; m is the predation rate; $\chi > 0$ (< 0) is the perceptual diffusion rate which implies that the consumer follows an attractive (repulsive) movement to the high-density area based on the perception of the population density; d is the natural death rate of the consumer.

According to [41], the perceptual function $q(x, t)$ is a cognitive map based on the learning and memory waning of the consumer and satisfies either of the following two ODEs:

$$\begin{aligned} \text{H1: } q_t &= bu - \gamma q, \\ \text{H2: } q_t &= buv - (\gamma + \xi v)q. \end{aligned}$$

When the cognitive map $q(x, t)$ satisfies (H1), then (1.2) becomes

$$(1.3) \quad \begin{cases} u_t = d_1 \Delta u + u \left(1 - \frac{u}{k}\right) - \frac{muv}{1+u}, & x \in \Omega, t > 0, \\ v_t = d_2 \Delta v - \chi \nabla \cdot (v \nabla q) + \frac{muv}{1+u} - dv, & x \in \Omega, t > 0, \\ q_t = bu - \gamma q, & x \in \Omega, t > 0, \\ \partial_\nu u = \partial_\nu v = 0, & x \in \partial\Omega, t > 0, \end{cases}$$

where the growth of $q(x, t)$ follows a constant proportion $b > 0$ to resource density, and $q(x, t)$ has a linear decay rate $\gamma > 0$. The model reveals that consumers can detect the local resource density and remember where they have previously found resources. When $q(x, t)$ satisfies (H2), (1.2) becomes the following system:

$$(1.4) \quad \begin{cases} u_t = d_1 \Delta u + u \left(1 - \frac{u}{k}\right) - \frac{muv}{1+u}, & x \in \Omega, t > 0, \\ v_t = d_2 \Delta v - \chi \nabla \cdot (v \nabla q) + \frac{muv}{1+u} - dv, & x \in \Omega, t > 0, \\ q_t = buv - (\gamma + \xi v)q, & x \in \Omega, t > 0, \\ \partial_\nu u = \partial_\nu v = 0, & x \in \partial\Omega, t > 0, \end{cases}$$

where the growth of $q(x, t)$ is assumed to have an additional decay at rate $\xi > 0$ when consumers return to an area and find a low resource density. Also, consumers may be able to share knowledge between individuals such that a location with high resource density is more likely to be remembered by consumers at the rate $bu(x, t)$. The assumption in model (1.4) is more reasonable than (1.3) because spatial memory is normally gained via interactive learning.

In model (1.3)/(1.4), the cognitive map is assumed to be a dynamically changing quantity, which continuously updates as consumers move around throughout their habitat and their memories are continuously formed and reformed over time. From the mathematical perspective, a dynamic cognitive map increases the mathematical complexity significantly as the description of movement for consumers may require a second ordinary differential equation (ODE) (H1) or (H2). Furthermore, it is known that diffusion has a regularizing effect, and thus the lack of diffusion in the equation of $q(x, t)$ brings more challenges to the analysis of system (1.3)/(1.4) than a classical reaction-diffusion system.

To the best of our knowledge, it has been challenging and in most cases impossible to directly connect the study of animals' cognition and memory on their spatial movement to biological data because the cognitive process should be described by information data in the brain of an organism. However, we find a handful of supporting

pieces of evidence from the works of experts in animal cognitive behavior; for example, certain brain functions or some other proxy has been empirically observed in the literature [7, 36, 37]. The main gap is how to build up a relation between these observations and the explicit cognitive behaviors (empirical data) of a species. Hypothesis testing via theoretical modeling is almost the only approach so far. The proposed models in this paper offer insightful qualitative movement behaviors and test key hypotheses on cognitive animal movements. This work lays a foundation for future theoretical studies and empirical data collection of cognitive movement mechanisms in driving resource-consumer dynamics.

In systems (1.3) and (1.4), we find that steady-state bifurcation and Hopf bifurcation can both occur such that the constant steady state is stable for a weak perceptual diffusion (either attractive or repulsive), while a strong perceptual diffusion can destabilize the systems and induce rich spatial patterns. In addition, the interaction between different modes of Hopf bifurcations in system (1.4) makes the system have more complex dynamical behaviors than (1.3). Biologically, one may expect a more diverse resource/consumer distribution if the consumers have a local perception described by (H2).

This paper is organized as follows. We investigate the dynamics and bifurcation of system (1.3) in section 2 with a description of the spectrum of the linearized operator at the constant steady state. In section 3, system (1.4) is investigated similarly to section 2. Finally, we conclude and discuss our work in section 4 and compare the two models studied in sections 2 and 3. In the paper, the space of measurable functions for which the p th power of the absolute value is Lebesgue integrable defined on a bounded and smooth domain $\Omega \subseteq \mathbb{R}^m$ is denoted by $L^p(\Omega)$. We use $W^{k,p}(\Omega)$ to denote the real-valued Sobolev space based on $L^p(\Omega)$ space. We denote by \mathbb{N} the set of all the positive integers and $\mathbb{N}_0 = \mathbb{N} \cup \{0\}$. Also, λ_n satisfying $0 = \lambda_0 < \lambda_1 < \dots < \lambda_{n-1} < \lambda_n < \dots < +\infty$ are the eigenvalues of the equation

$$\begin{cases} \Delta\phi(x) + \lambda\phi(x) = 0, & x \in \Omega, \\ \partial_\nu\phi(x) = 0, & x \in \partial\Omega, \end{cases}$$

with the corresponding eigenfunctions $\phi_n(x) > 0$ satisfying $\int_\Omega \phi_n^2(x)dx = 1$.

2. The dynamics of model (1.3). In this section, we study the dynamics of system (1.2) with cognitive map $q(x, t)$ satisfying (H1), i.e., model (1.3), which has a constant equilibrium $(u, v, q) = (\theta, v_\theta, q_\theta)$ with

$$\theta = \frac{d}{m-d}, v_\theta = \frac{(k-\theta)(1+\theta)}{km}, q_\theta = \frac{b\theta}{\gamma},$$

provided that

$$(2.1) \quad m > d, k > \theta.$$

By a standard calculation, the linearized Jacobian matrix of the kinetic system of (1.3) at $(\theta, v_\theta, q_\theta)$ is

$$J = \begin{pmatrix} \beta & -d & 0 \\ \alpha & 0 & 0 \\ b & 0 & -\gamma \end{pmatrix},$$

where

$$(2.2) \quad \alpha = \frac{k-\theta}{k(1+\theta)}, \beta = \frac{\theta(k-1-2\theta)}{k(1+\theta)}.$$

One can easily verify that all the eigenvalues of J have negative real parts when $k < 1 + 2\theta$ such that $(\theta, v_\theta, q_\theta)$ is locally asymptotically stable concerning the kinetic system. Note that $k = 1 + 2\theta$ is the critical value for the kinetic system to undergo a Hopf bifurcation near $(\theta, v_\theta, q_\theta)$. Together with (2.1), we always assume the following conditions hold:

(A) $m > d, \theta < k < 1 + 2\theta,$

such that $(\theta, v_\theta, q_\theta)$ is locally asymptotically stable concerning the kinetic system of (1.3). In the following, we investigate the stability of the constant steady state $(\theta, v_\theta, q_\theta)$ under assumption (A) and carry a bifurcation analysis for system (1.3).

2.1. Spectrum of the linearized operator. In this part, we perform a spectral analysis of the linearized operator at the constant steady state $(\theta, v_\theta, q_\theta)$ via the methods in [3, 14, 16]. Define

$$(2.3) \quad X = W_N^{2,p}(\Omega) \times W_N^{2,p}(\Omega) \times W^{2,p}(\Omega), Y = L^p(\Omega) \times L^p(\Omega) \times W_N^{2,p}(\Omega),$$

where

$$W_N^{2,p}(\Omega) = \{u \in W^{2,p}(\Omega) : \partial_\nu u = 0 \text{ on } \partial\Omega\}.$$

We linearize (1.3) at $(\theta, v_\theta, q_\theta)$ and obtain the linear operator

$$(2.4) \quad \mathcal{L} \begin{pmatrix} \phi \\ \psi \\ \varphi \end{pmatrix} = \begin{pmatrix} d_1 \Delta \phi + \beta \phi - d\psi \\ d_2 \Delta \psi - \chi v_\theta \Delta \varphi + \alpha \phi \\ b\phi - \gamma \varphi \end{pmatrix},$$

where \mathcal{L} is a closed linear operator with domain $D(\mathcal{L}) = X$, which implies that $\phi \in W_N^{2,p}(\Omega), \psi \in W_N^{2,p}(\Omega),$ and $\varphi \in W^{2,p}(\Omega).$ In the following, we provide the results about the spectrum of $\mathcal{L}.$

THEOREM 2.1. *Let $\mathcal{L} : X \rightarrow Y$ be defined as in (2.4). Then the spectrum of \mathcal{L} is*

$$\sigma(\mathcal{L}) = \sigma_p(\mathcal{L}) = S \cup \{-\gamma\},$$

where

$$(2.5) \quad S = \{\mu_n^{(1)}\}_{n=0}^{+\infty} \cup \{\mu_n^{(2)}\}_{n=0}^{+\infty} \cup \{\mu_n^{(3)}\}_{n=0}^{+\infty}.$$

Here $\mu_n^{(j)}, j = 1, 2, 3,$ satisfying $\text{Re}(\mu_n^{(1)}) < \text{Re}(\mu_n^{(2)}) < \text{Re}(\mu_n^{(3)})$ are the roots of the following characteristic equation:

$$(2.6) \quad \mu^3 + A_n \mu^2 + B_n \mu + C_n = 0, \quad n \in \mathbb{N}_0,$$

where

$$\begin{aligned} A_n &= (d_1 + d_2)\lambda_n - \beta + \gamma, \\ B_n &= d_2 \lambda_n (d_1 \lambda_n - \beta) + \gamma (d_1 \lambda_n + d_2 \lambda_n - \beta) + d\alpha, \\ C_n &= \gamma d_2 \lambda_n (d_1 \lambda_n - \beta) + b d \chi v_\theta \lambda_n + \gamma d \alpha. \end{aligned}$$

Proof. In order to analyze the spectrum of \mathcal{L} defined as in (2.4), we consider the following nonhomogeneous problem:

$$(2.7) \quad \begin{cases} d_1 \Delta \phi + \beta \phi - d\psi = \mu \phi + \tau_1, \\ d_2 \Delta \psi - \chi v_\theta \Delta \varphi + \alpha \phi = \mu \psi + \tau_2, \\ b\phi - \gamma \varphi = \mu \varphi + \tau_3, \\ \partial_\nu \phi = \partial_\nu \psi = 0, \end{cases}$$

where $\mu \in \mathbb{C}$ and $(\tau_1, \tau_2, \tau_3) \in Y$. There are the following two cases according to the solution of the third equation in (2.7).

Case 1: $\mu \neq -\gamma$. From the third equation of (2.7), we obtain $\varphi = \frac{b\phi - \tau_3}{\mu + \gamma}$ and, substituting it into the second equation, we have

$$\begin{cases} d_1 \Delta \phi + \beta \phi - d\psi = \mu \phi + \tau_1, \\ d_2 \Delta \psi - \frac{\chi v_\theta}{\mu + \gamma} (b \Delta \phi - \Delta \tau_3) + \alpha \phi = \mu \psi + \tau_2, \\ \partial_\nu \phi = \partial_\nu \psi = 0, \end{cases}$$

which is equivalent to

$$(2.8) \quad \mathcal{L}_1 \begin{pmatrix} \phi \\ \psi \end{pmatrix} = \begin{pmatrix} d_1 \Delta \phi + \beta \phi - d\psi - \mu \phi \\ d_2 \Delta \psi - \frac{b\chi v_\theta}{\mu + \gamma} \Delta \phi + \alpha \phi - \mu \psi \end{pmatrix} = \begin{pmatrix} \tau_1 \\ \tau_2 - \frac{\chi v_\theta}{\mu + \gamma} \Delta \tau_3 \end{pmatrix}.$$

As $\phi, \psi \in W_N^{2,p}(\Omega)$ from (2.4), and the eigenfunctions $\{\phi_n\}_{n=0}^{+\infty}$ of $-\Delta$ form a complete and orthonormal basis for $W_N^{2,p}(\Omega)$, thus we set

$$(2.9) \quad \phi = \sum_{n=0}^{+\infty} a_n \phi_n, \quad \psi = \sum_{n=0}^{+\infty} b_n \phi_n.$$

Substituting (2.9) into (2.8), multiplying the equation by ϕ_n , and integrating it over Ω , we obtain

$$\begin{pmatrix} -d_1 \lambda_n + \beta - \mu & -d \\ \frac{b\chi v_\theta \lambda_n}{\mu + \gamma} + \alpha & -d_2 \lambda_n - \mu \end{pmatrix} \begin{pmatrix} a_n \\ b_n \end{pmatrix} = \begin{pmatrix} \int_{\Omega} \tau_1 dx \\ \int_{\Omega} \left(\tau_2 - \frac{\chi v_\theta}{\mu + \gamma} \Delta \tau_3 \right) dx \end{pmatrix}.$$

By letting $\tau_1 = \tau_2 = \tau_3 = 0$, we obtain that $\text{Ker}(\mathcal{L}_1) = \{(0, 0)^T\}$, which implies that $\text{Ker}(\mathcal{L} - \mu I) = \{(0, 0, 0)^T\}$ and the operator $\mathcal{L} - \mu I$ is injective when the following condition holds:

$$\begin{vmatrix} -d_1 \lambda_n + \beta - \mu & -d \\ \frac{b\chi v_\theta \lambda_n}{\mu + \gamma} + \alpha & -d_2 \lambda_n - \mu \end{vmatrix} \neq 0,$$

which is equivalent to

$$(2.10) \quad (\mu + d_1 \lambda_n - \beta)(\mu + d_2 \lambda_n)(\mu + \gamma) + bd\chi v_\theta \lambda_n + d\alpha(\mu + \gamma) \neq 0.$$

From (2.7), we can obtain that $\text{Ran}(\mathcal{L} - \mu I) = L^p(\Omega) \times L^p(\Omega) \times W_N^{2,p}(\Omega) = Y$, which implies that $\mathcal{L} - \mu I$ is surjective. By the open mapping theorem (Theorem 5.8 in [39]) and the fact that $\mathcal{L} - \mu I$ is bijective, we know that $(\mathcal{L} - \mu I)^{-1}$ is bounded with

$$\begin{aligned} & \|\phi\|_{W_N^{2,p}(\Omega)} + \|\psi\|_{W_N^{2,p}(\Omega)} \\ & \leq \|(\mathcal{L} - \mu I)^{-1}\| \left(\|d_1 \Delta \phi + \beta \phi - d\psi\|_{L^p(\Omega)} + \left\| d_2 \Delta \psi - \frac{b\chi v_\theta}{\mu + \gamma} \Delta \phi + \alpha \phi \right\|_{L^p(\Omega)} \right), \end{aligned}$$

which directly results from the boundedness of $(\mathcal{L} - \mu I)^{-1}$. Therefore, we know that μ belongs to the resolvent set of \mathcal{L} and is not in the spectrum set when inequality (2.10) holds.

If (2.10) does not hold, then the dispersal relation in (2.6) holds and has three roots, $\mu_n^{(j)}$, $j = 1, 2, 3$, for each $n \in \mathbb{N}_0$. For $j = 1, 2, 3$, we put $\mu = \mu_n^{(j)}$ into (2.7) and set $\tau_1 = \tau_2 = \tau_3 = 0$. Then it can be obtained that

$$\begin{pmatrix} \phi \\ \psi \\ \varphi \end{pmatrix} = \begin{pmatrix} \phi^{(j)} \\ \psi^{(j)} \\ \varphi^{(j)} \end{pmatrix} = \begin{pmatrix} 1 \\ \frac{1}{d}(-d_1\lambda_n + \beta - \mu_n^{(j)}) \\ \frac{b}{\mu_n^{(j)} + \gamma} \end{pmatrix} \phi_n,$$

which implies that $Ker(\mathcal{L} - \mu_n^{(j)}I) = Span\{(\phi^{(j)}, \psi^{(j)}, \varphi^{(j)})^T\}$. Therefore, we know that $\mu_n^{(j)}$, $j = 1, 2, 3$, are the eigenvalues of \mathcal{L} and $\mu_n^{(j)} \in \sigma_p(\mathcal{L})$, which denotes the set of point spectrum of \mathcal{L} .

Case 2: $\mu = -\gamma$. In this case, (2.7) can be solved as

$$\begin{cases} \psi = \frac{1}{bd}(d_1\Delta\tau_3 + \beta\tau_3 + \gamma\tau_3 - b\tau_1), \\ \Delta\varphi = \frac{1}{b\chi v_\theta}(-b\gamma\psi + \tau_2 - \alpha\tau_3 - bd_2\Delta\psi). \end{cases}$$

By letting $\tau_1 = \tau_2 = \tau_3 = 0$, we obtain $Ker(\mathcal{L} + \gamma I) = Span\{(0, 0, \tilde{\varphi})^T\}$, with $\tilde{\varphi}$ satisfying $\Delta\tilde{\varphi} = 0$, and thus $-\gamma \in \sigma_p(\mathcal{L})$. This completes the proof. \square

Based on the spectrum analysis in Theorem 2.1, we obtain the following results to determine the stability of the constant equilibrium for (1.3).

COROLLARY 2.2. *The constant equilibrium $(\theta, v_\theta, q_\theta)$ of (1.3) is locally stable when all the roots of the characteristic equation (2.6) have negative real parts; otherwise it is unstable.*

Proof. From Theorem 2.1, we see that the spectrum of the linearized operator \mathcal{L} corresponding to the linearized system of (1.3) at $(\theta, v_\theta, q_\theta)$ is $\sigma(\mathcal{L}) = \sigma_p(\mathcal{L}) = S \cup \{-\gamma\}$. Note that the linear stability of $(\theta, v_\theta, q_\theta)$ implies its nonlinear stability according to [10] as the spectral set is discrete. Since $-\gamma \in \mathbb{C}^-$, thus it can be inferred that the stability of $(\theta, v_\theta, q_\theta)$ is determined by the set S , which consists of the roots of (2.6), and we reach our conclusion. \square

2.2. Bifurcation analysis. From Theorem 2.1 and Corollary 2.2, we know that the stability of the constant steady state $(\theta, v_\theta, q_\theta)$ of system (1.3) can be determined by the characteristic equation (2.6). By the Routh–Hurwitz stability criterion, all the eigenvalues of (2.6) have negative real parts if and only if

$$A_n > 0, C_n > 0, A_n B_n - C_n > 0.$$

Under assumption (A), we have $\alpha > 0, \beta < 0$ with α, β defined by (2.2), which will be applied in the calculations throughout the whole section. From $\beta < 0$, we know that $A_n > 0$ always holds and the real parts of the eigenvalues of (2.6) may change sign either via $C_n = 0$ (which implies (2.6) has a zero root) or via $A_n B_n - C_n = 0$ (which implies (2.6) has a pair of purely imaginary roots). Also, we can observe that $B_n > 0$ always holds as $\beta < 0, \alpha > 0$, so $C_n = 0$ and $A_n B_n - C_n = 0$ cannot occur at the same time.

Taking χ and γ as the bifurcation parameters, we obtain the steady-state bifurcation points by solving $C_n = 0$,

$$(2.11) \quad \chi_n^S(\gamma) = -\frac{\gamma k d_2 \lambda_n (d_1 \lambda_n - \beta) + \gamma d \alpha}{b d v_\theta \lambda_n},$$

and the Hopf bifurcation points by solving $A_n B_n - C_n = 0$,

$$(2.12) \quad \chi_n^H(\gamma) = \frac{((d_1 + d_2)\lambda_n - \beta) [\gamma^2 + \gamma((d_1 + d_2)\lambda_n - \beta) + d_2\lambda_n(d_1\lambda_n - \beta) + d\alpha]}{bdv_\theta\lambda_n}.$$

LEMMA 2.3. *Let $\chi_n^S(\gamma)$ and $\chi_n^H(\gamma)$ be defined as in (2.11) and (2.12), respectively. Then the following statements are true under assumption (A):*

- (i) *For fixed $n \in \mathbb{N}$, $\chi_n^S(\gamma)$ is strictly decreasing with respect to γ and passes through the origin, and it is also known that $\chi_n^S(0) = 0$ and $\lim_{\gamma \rightarrow +\infty} \chi_n^S(\gamma) = -\infty$. Also, $\chi_n^H(\gamma)$ is strictly increasing with respect to γ and $\chi_n^H(\gamma) > 0$.*
- (ii) *For fixed $\gamma > 0$, there exists $N, M \in \mathbb{N}$ such that $\chi_N^S(\gamma) = \max_{n \in \mathbb{N}} \chi_n^S(\gamma) < 0$ and $\chi_M^H(\gamma) = \min_{n \in \mathbb{N}} \chi_n^H(\gamma) > 0$.*

Proof. By the definition of $\chi_n^S(\gamma)$ given in (2.11), it is easy to see that $\chi_n^S(\gamma)$ is a straight line passing through the origin with the slope

$$K_n = -\frac{1}{bdv_\theta} \left(d_1 d_2 \lambda_n + \frac{d\alpha}{\lambda_n} - d_2 \beta \right) < 0.$$

Then we immediately obtain the results about $\chi_n^S(\gamma)$ in (i). Also, it is clear from (2.12) that $\chi_n^H(\gamma)$ is a quadratic function of γ and can be rewritten as $\chi_n^H(\gamma) = a_2\gamma^2 + a_1\gamma + a_0$ with

$$a_2 = \frac{(d_1 + d_2)\lambda_n - \beta}{bdv_\theta\lambda_n}, \quad a_1 = \frac{((d_1 + d_2)\lambda_n - \beta)^2}{bdv_\theta\lambda_n},$$

$$a_0 = \frac{((d_1 + d_2)\lambda_n - \beta)d_2\lambda_n(d_1\lambda_n - \beta) + d\alpha}{bdv_\theta\lambda_n}.$$

Immediately, we obtain that $a_2 > 0$, $a_1 > 0$, $a_0 > 0$ and the symmetrical axis $\gamma = -\frac{a_1}{2a_2} < 0$. Thus, it can be inferred that $\chi_n^H(\gamma)$ is increasing for $\gamma > 0$. By the fact that $\chi_n^H(0) = a_0 > 0$, we know that $\chi_n^H(\gamma) > 0$ for all $\gamma > 0$.

For (ii), we see that K_n is a hook function of λ_n , and thus it can be known that K_n reaches its maximum at $\lambda_n = \sqrt{\frac{d\alpha}{d_1 d_2}}$. We may choose N such that λ_N is the closest eigenvalue to $\sqrt{\frac{d\alpha}{d_1 d_2}}$. From (i), we see that $\chi_n^S(\gamma) < 0$ for any $\gamma > 0$; then it is natural that $\chi_N^S(\gamma) < 0$. To prove the existence of $\chi_M^H(\gamma)$, we first rewrite $\chi_n^H(\gamma)$ as the following form by replacing λ_n by a continuous variable p :

$$(2.13) \quad \chi_p^H(\gamma) = \frac{((d_1 + d_2)p - \beta) [\gamma^2 + \gamma(d_1 p + d_2 p - \beta) + d_2 p(d_1 p - \beta) + d\alpha]}{bdv_\theta p}.$$

By differentiating $\chi_p^H(\gamma)$ with respect to p , we have

$$\frac{d[\chi_p^H(\gamma)]}{dp} = \frac{1}{bdv_\theta p^2} [2(d_1 + d_2)d_1 d_2 p^3 + ((d_1 + d_2)^2 \gamma - \beta(2d_1 d_2 + d_2^2))p^2 + \beta\gamma^2 - \beta^2 \gamma + \beta d\alpha].$$

Let

$$f(p) = 2(d_1 + d_2)d_1 d_2 p^3 + ((d_1 + d_2)^2 \gamma - \beta(2d_1 d_2 + d_2^2))p^2 + \beta\gamma^2 - \beta^2 \gamma + \beta d\alpha.$$

Then one can verify that $f(p)$ has a unique positive zero $p = p_*$ as

$$f'(p) = 6(d_1 + d_2)d_1d_2p^2 + 2((d_1 + d_2)^2\gamma - \beta(2d_1d_2 + d_2^2))p > 0 \text{ for } p > 0,$$

and $f(0) = \beta\gamma^2 - \beta^2\gamma + \beta d\alpha < 0$, $\lim_{p \rightarrow +\infty} f(p) = +\infty$. Also we found that $f(p) > 0$ for $p \in (p_*, +\infty)$ and $f(p) < 0$ for $p \in (0, p_*)$, which implies that $\frac{d[\chi_p^H(\gamma)]}{dp} > 0$ for $p \in (p_*, +\infty)$ and $\frac{d[\chi_p^H(\gamma)]}{dp} < 0$ for $p \in (0, p_*)$ and $\chi_p^H(\gamma)$ reaches its minimum at $p = p_*$. By the relation that $p = \lambda_n$, we know that there must exist an $M \in \mathbb{N}$ such that λ_M is the closest eigenvalue to p_* and $\chi_M^H(\gamma) = \min_{n \in \mathbb{N}} \chi_n^H(\gamma)$. \square

LEMMA 2.4. Let $\chi_N^S(\gamma)$ and $\chi_M^H(\gamma)$ be defined as in Lemma 2.3:

- (i) When $\chi < \chi_N^S(\gamma) < \chi < \chi_M^H(\gamma)$, all the eigenvalues of (2.6) have negative real parts.
- (ii) When $\chi \geq \chi_M^H(\gamma)$, (2.6) has a pair of purely imaginary roots $\mu = \pm i\omega_n$ with $\omega_n > 0$ if $\chi = \chi_n^H(\gamma)$.
- (iii) When $\chi \leq \chi_N^S(\gamma)$, (2.6) has a root $\mu = 0$ if $\chi = \chi_n^S(\gamma)$.

Proof. From Lemma 2.3, when $\chi_N^S(\gamma) < \chi < \chi_M^H(\gamma)$, we have $C_n > 0$ and $A_n B_n - C_n > 0$ for all $\lambda_n > 0$ so all the eigenvalues of (2.6) have negative real parts for all $n \in \mathbb{N}_0$. When $\chi \leq \chi_N^S(\gamma)$, we have $C_n < 0$, so the characteristic equation (2.6) has at least one eigenvalue with positive real part, and when $\chi = \chi_n^S(\gamma)$, (2.6) has a zero eigenvalue. When $\chi \geq \chi_M^H(\gamma)$, we have $A_n > 0$, $C_n > 0$ but $A_n B_n - C_n < 0$, so not all the eigenvalues of (2.6) have negative real parts. In particular, when $\chi = \chi_n^H(\gamma)$, (2.6) has a pair of complex eigenvalues with zero real part. \square

From Lemma 2.4, we know that (2.6) has a pair of purely imaginary eigenvalues $\pm i\omega_n$ ($\omega_n > 0$) when $\chi = \chi_n^H(\gamma)$. The following lemma shows that the transversality condition holds at $\chi = \chi_n^H(\gamma)$.

LEMMA 2.5. Let $\chi = \chi_n^H(\gamma)$ be defined as in (2.12). Then (2.6) has a pair of roots in the form $\mu = \eta(\chi) \pm i\omega(\chi)$ when χ is near $\chi_n^H(\gamma)$ such that $\eta(\chi_n^H(\gamma)) = 0$ and $\eta'(\chi_n^H(\gamma)) > 0$.

Proof. We mainly prove that $\eta'(\chi_n^H(\gamma)) > 0$. Differentiating (2.6) with respect to χ , we have

$$(2.14) \quad 3\mu^2 \frac{d\mu}{d\chi} + \frac{dA_n}{d\chi} \mu^2 + 2A_n \mu \frac{d\mu}{d\chi} + \frac{dB_n}{d\chi} \mu + B_n \frac{d\mu}{d\chi} + \frac{dC_n}{d\chi} = 0.$$

From the expressions of A_n, B_n, C_n in (2.6), it is straightforward to see that

$$(2.15) \quad \frac{dA_n}{d\chi} = 0, \frac{dB_n}{d\chi} = 0, \frac{dC_n}{d\chi} = b d v_\theta \lambda_n.$$

Substituting (2.15), $\mu = i\omega_n$, $B_n = \omega_n^2$, and $\chi = \chi_n^H(\gamma)$ into (2.14), we obtain

$$\frac{d\mu}{d\chi} \Big|_{\chi=\chi_n^H(\gamma)} = \frac{b d v_\theta \lambda_n}{2\omega_n^2 - 2i\omega_n A_n},$$

and thus

$$\eta'(\chi) = \text{Re} \left(\frac{d\mu}{d\chi} \Big|_{\chi=\chi_n^H(\gamma)} \right) = \frac{b d v_\theta \lambda_n}{2(\omega_n^2 + A_n^2)} > 0. \quad \square$$

By Lemmas 2.3, 2.4, and 2.5 and Hopf bifurcation theory for partial functional differential equations, we obtain the following results on the stability and bifurcation behaviors of the positive homogeneous steady state of (1.3).

Downloaded 05/13/24 to 137.186.145.70 . Redistribution subject to SIAM license or copyright; see https://pubs.siam.org/terms-privacy

THEOREM 2.6. *Assume that the conditions in (A) hold, and let $\chi_n^S(\gamma)$, $\chi_n^H(\gamma)$ be defined as in (2.11), (2.12) and $\chi_N^S(\gamma), \chi_M^H(\gamma)$ in Lemma 2.3. Then we have the following results for (1.3):*

- (i) *A mode- n Turing bifurcation occurs at $\chi = \chi_n^S(\gamma)$ for $\gamma > 0$ and $n \in \mathbb{N}$; thus a mode- n spatially nonhomogeneous steady state can arise near $(\theta, v_\theta, q_\theta)$.*
- (ii) *A mode- n Hopf bifurcation occurs at $\chi = \chi_n^H(\gamma)$ for $\gamma > 0$ and $n \in \mathbb{N}$, and the bifurcating periodic solutions are spatially nonhomogeneous.*
- (iii) *For a fixed $\gamma \in (0, +\infty)$, the positive homogeneous steady state $(\theta, v_\theta, q_\theta)$ is locally asymptotically stable for $\chi_N^S(\gamma) < \chi < \chi_M^H(\gamma)$ and unstable for $\chi \in (-\infty, \chi_N^S(\gamma)] \cup [\chi_M^H(\gamma), +\infty)$.*

Here “a mode- n Turing/Hopf bifurcation” implies that the corresponding bifurcation curve is associated with wave number n , which results from the eigenvalues λ_n of $-\Delta$ in the characteristic equation (2.6). On one-dimensional spatial domain $\Omega = (0, \pi)$, the bifurcation diagram of (1.3) is illustrated in Figure 1 by taking the parameters as $d_1 = 0.01$, $d_2 = 0.03$, $m = 1$, $d = 0.1$, $k = 1$, $b = 0.15$. In the following, we perform some numerical simulations based on the following initial conditions:

- (I1) $u_0(x) = \theta - 0.01 \cos(x)$, $v_0(x) = v_\theta - 0.01 \cos(x)$, $q_0(x) = q_\theta - 0.1 \cos(x)$,
- (I2) $u_0(x) = \theta - 0.01 \cos(2x)$, $v_0(x) = v_\theta - 0.01 \cos(2x)$, $q_0(x) = q_\theta - 0.1 \cos(2x)$,
- (I3) $u_0(x) = \theta - 0.01 \cos(3x)$, $v_0(x) = v_\theta - 0.01 \cos(3x)$, $q_0(x) = q_\theta - 0.1 \cos(3x)$,
- (I4) $u_0(x) = \theta - 0.01 \cos(4x)$, $v_0(x) = v_\theta - 0.01 \cos(4x)$, $q_0(x) = q_\theta - 0.1 \cos(4x)$,

and we will indicate the initial conditions (IC) for each figure. Note that we only demonstrate the distribution of resources in each figure as the consumers always follow the resources and have similar spatial distribution.

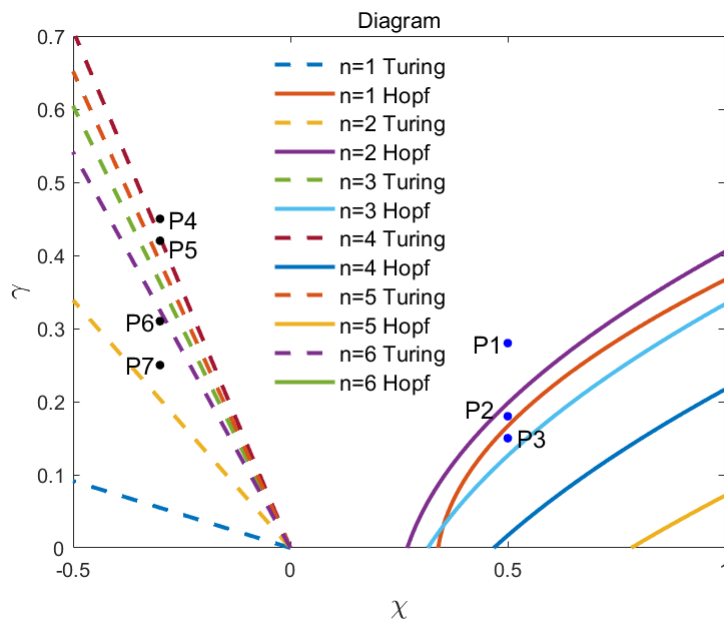


FIG. 1. *The bifurcation diagram of system (1.3) in the (χ, γ) plane with $d_1 = 0.01$, $d_2 = 0.03$, $m = 1$, $d = 0.1$, $k = 1$, $b = 0.15$, $\Omega = (0, \pi)$, and the Turing bifurcation curves $\chi = \chi_n^S(\gamma)$ defined as in (2.11) can be identified by the dashed curves and the Hopf bifurcation curves $\chi = \chi_n^H(\gamma)$ defined as in (2.12) by the solid curves. The points are parameter values for the numerical simulations, and they are P1 (0.5, 0.28), P2 (0.5, 0.18), P3 (0.5, 0.15), P4 (−0.3, 0.45), P5 (−0.3, 0.42), P6 (−0.3, 0.31), and P7 (−0.3, 0.25).*

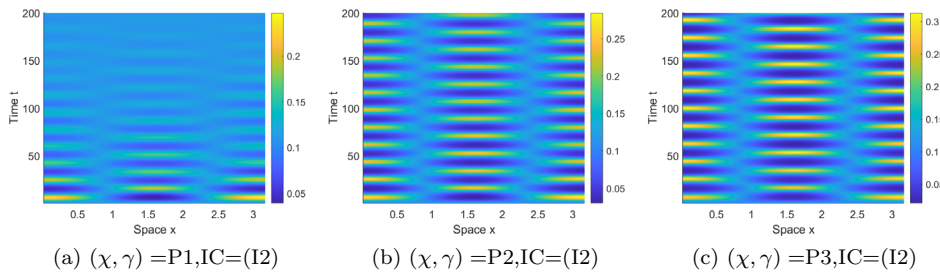


FIG. 2. Periodic patterns arising near Hopf bifurcation curves in system (1.3) when parameters are $d_1 = 0.01$, $d_2 = 0.03$, $m = 1$, $d = 0.1$, $k = 1$, $b = 0.15$, and $\Omega = (0, \pi)$. Here, P1, P2, P3 are the parameter value points in the diagram plane in Figure 1. In each figure, the color indicates the value of $u(x, t)$ according to the color bar.

From Figure 1, we observe that the mode-2 Hopf curve is the first Hopf curve, and then we choose some points near the Hopf bifurcation curves to observe periodic patterns in system (1.3). In Figure 2, for fixed $\chi = 0.5$, we observe that the steady state $(\theta, v_\theta, q_\theta)$ is stable when $\gamma = 0.28$ (corresponding to P1, which is in the stable region). When we decrease γ to 0.18 (corresponding to P2, which is under the first Hopf bifurcation curve), it is shown that a mode-2 spatially nonhomogeneous periodic pattern arises. When $\gamma = 0.15$, the mode-2 spatially nonhomogeneous periodic pattern remains stable as the mode-2 Hopf bifurcation curve is the dominant Hopf bifurcation curve. In this situation, we see that the spatial distribution of resources will periodically change over time.

In Figure 3, we demonstrate the spatially nonhomogeneous steady state and some wandering periodic patterns when $\chi = -0.3$. When we choose $\gamma = 0.45$ corresponding to P4 in Figure 1, the constant steady state $(\theta, v_\theta, q_\theta)$ is stable, as shown in (a). If we decrease γ to 0.42 corresponding to P5, which is below the mode-4 Turing curve, it is shown that a mode-4 spatially nonhomogeneous steady state arises, as illustrated in (b). This situation happens when the environment of the living habitat is steady over time so that resources and consumers can keep their dynamic balance. When we continue to decrease the γ value, we observe some “wandering” patterns with large periods, as shown in (c) and (d), which demonstrate a distinguished distribution of resources from the periodic patterns (see Figure 2) induced by Hopf bifurcation. These patterns are also observed in previous work of the Keller–Segel chemotaxis model with growth [20] and distributed spatial memory [28].

3. The dynamics of model (1.4). In this section, we investigate the dynamics of system (1.4). Under assumption (A), (1.4) admits a positive equilibrium $(\theta, v_\theta, \tilde{q}_\theta)$, where

$$\theta = \frac{d}{m-d}, \quad v_\theta = \frac{(k-\theta)(1+\theta)}{km}, \quad \tilde{q}_\theta = \frac{b\theta v_\theta}{\gamma + \xi v_\theta},$$

which is locally asymptotically stable concerning the kinetic system.

Linearizing (1.4) at $(\theta, v_\theta, \tilde{q}_\theta)$ leads to the linear operator

$$(3.1) \quad \tilde{\mathcal{L}} \begin{pmatrix} \phi \\ \psi \\ \varphi \end{pmatrix} = \begin{pmatrix} d_1 \Delta \phi + \beta \phi - d\psi \\ d_2 \Delta \psi - \chi v_\theta \Delta \varphi + \alpha \phi \\ b\theta \phi + \frac{b\theta \gamma}{\gamma + \xi v_\theta} \psi - (\gamma + \xi v_\theta) \varphi \end{pmatrix},$$

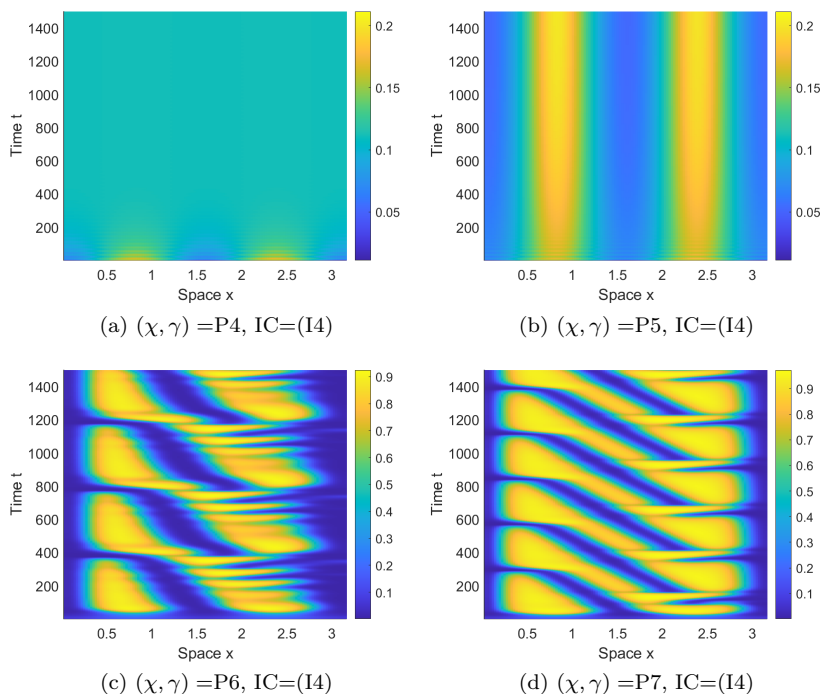


FIG. 3. Spatial patterns arising near Turing bifurcation curves in system (1.3) when parameters are $d_1 = 0.01$, $d_2 = 0.03$, $m = 1$, $d = 0.1$, $k = 1$, $b = 0.15$, and $\Omega = (0, \pi)$. In each figure, the color indicates the value of $u(x, t)$ according to the color bar.

where $\alpha > 0$, $\beta < 0$ are defined as in (2.2). Then we know that $\tilde{\mathcal{L}}$ is a closed linear operator in Y with domain $D(\tilde{\mathcal{L}}) = X$ with X, Y defined as in (2.3). In the following, we provide the results about the spectrum of $\tilde{\mathcal{L}}$.

THEOREM 3.1. Let $\tilde{\mathcal{L}} : X \rightarrow Y$ be defined as in (3.1). Then the spectrum of $\tilde{\mathcal{L}}$ is

$$\sigma(\tilde{\mathcal{L}}) = \sigma_p(\tilde{\mathcal{L}}) = \tilde{S} \cup \{-\gamma - \xi v_\theta\},$$

where

$$(3.2) \quad \tilde{S} = \{\tilde{\mu}_n^{(1)}\}_{n=0}^\infty \cup \{\tilde{\mu}_n^{(2)}\}_{n=0}^\infty \cup \{\tilde{\mu}_n^{(3)}\}_{n=0}^\infty,$$

where $\tilde{\mu}_n^{(j)}$, $j = 1, 2, 3$, satisfying $\text{Re}(\tilde{\mu}_n^{(1)}) < \text{Re}(\tilde{\mu}_n^{(2)}) < \text{Re}(\tilde{\mu}_n^{(3)})$ are the roots of the following characteristic equation:

$$(3.3) \quad \mu^3 + \tilde{A}_n \mu^2 + \tilde{B}_n \mu + \tilde{C}_n = 0, \quad n \in \mathbb{N}_0,$$

with

$$\tilde{A}_n = (d_1 + d_2)\lambda_n - \beta + \gamma + \xi v_\theta,$$

$$\tilde{B}_n = d_2 \lambda_n (d_1 \lambda_n - \beta) + (\gamma + \xi v_\theta)(d_1 \lambda_n + d_2 \lambda_n - \beta) + \alpha - \frac{\chi b \theta v_\theta \gamma \lambda_n}{\gamma + \xi v_\theta},$$

$$\tilde{C}_n = (\gamma + \xi v_\theta) d_2 \lambda_n (d_1 \lambda_n - \beta) + b \theta v_\theta^2 \chi \lambda_n + d \alpha (\gamma + \xi v_\theta) - \frac{\chi b \theta v_\theta \gamma \lambda_n (d_1 \lambda_n - \beta)}{\gamma + \xi v_\theta}.$$

The proof of Theorem 3.1 is tedious, and thus we put the details in Appendix A. Similarly to the proof of Corollary 2.2, we obtain the following result.

COROLLARY 3.2. *In system (1.4), the constant equilibrium $(\theta, v_\theta, \tilde{q}_\theta)$ is locally stable when all the roots of the characteristic equation (3.3) have negative real parts; otherwise it is unstable.*

From Theorem 3.1 and Corollary 3.2, we know that the stability of the constant steady state $(\theta, v_\theta, \tilde{q}_\theta)$ of system (1.4) can be determined by the characteristic equation (3.3). The steady-state bifurcation points can be obtained by solving $\tilde{C}_n = 0$,

$$(3.4) \quad \tilde{\chi}_n^S(\gamma) = -\frac{(\gamma + \xi v_\theta)(d_2 \lambda_n (d_1 \lambda_n - \beta) + d\alpha)}{bdv_\theta^2 \lambda_n - (d_1 \lambda_n - \beta) \frac{b\theta \gamma v_\theta \lambda_n}{\gamma + \xi v_\theta}},$$

and the Hopf bifurcation points by solving $\tilde{A}_n \tilde{B}_n - \tilde{C}_n = 0$,

$$(3.5) \quad \tilde{\chi}_n^H(\gamma) = \frac{((d_1 + d_2)\lambda_n - \beta)}{bdv_\theta^2 \lambda_n + b\theta \gamma v_\theta \lambda_n + \frac{d_2 b \theta \gamma v_\theta \lambda_n^2}{\gamma + \xi v_\theta}} [d_2 \lambda_n (d_1 \lambda_n - \beta) + (\gamma + \xi v_\theta)((d_1 + d_2)\lambda_n - \beta) + (\gamma + \xi v_\theta)^2 + d\alpha].$$

In the following lemma, we give a detailed description of the properties of Turing curves $\chi = \tilde{\chi}_n^S(\gamma)$. For the convenience of writing, we define

$$(3.6) \quad \begin{aligned} Q_n(\gamma) &= (\gamma + \xi v_\theta)(d_2 \lambda_n (d_1 \lambda_n - \beta) + d\alpha), \\ P_n(\gamma) &= bdv_\theta^2 \lambda_n - (d_1 \lambda_n - \beta) \frac{b\theta \gamma v_\theta \lambda_n}{\gamma + \xi v_\theta}. \end{aligned}$$

LEMMA 3.3. *Let $\tilde{\chi}_n^S(\gamma)$ and $\tilde{\chi}_n^H(\gamma)$ be defined as in (3.4) and (3.5), respectively. Then the following statements are true:*

- (i) *There exists $n_* \in \mathbb{N}$ such that*
 - (a) *when $n \leq n_*$, $\tilde{\chi}_n^S(\gamma) < 0$ and there exists $N \in \mathbb{N}$ such that $\tilde{\chi}_N^S(\gamma) = \max_{n \in \mathbb{N}} \tilde{\chi}_n^S(\gamma)$ for a fixed $\gamma > 0$;*
 - (b) *when $n > n_*$, $\tilde{\chi}_n^S(\gamma) < 0$ for $\gamma \in (0, \gamma_n^*)$ and $\tilde{\chi}_n^S(\gamma) > 0$ for $\gamma \in (\gamma_n^*, +\infty)$ with γ_n^* satisfying $P_n(\gamma_n^*) = 0$; for a fixed $\gamma > 0$, $\tilde{\chi}_n^S(\gamma)$ is strictly decreasing with respect to n and satisfies*

$$(3.7) \quad \tilde{\chi}_n^S(\gamma) > \tilde{\chi}_\infty^S(\gamma) = \frac{d_2(\gamma + \xi v_\theta)^2}{b\theta \gamma v_\theta},$$

where $\tilde{\chi}_\infty^S(\gamma)$ is decreasing for $\gamma \in (0, \gamma_)$ and increasing for $\gamma \in (\gamma_*, +\infty)$ with $\gamma_* = \xi v_\theta$.*

- (ii) *There exists $M \in \mathbb{N}$ such that $\tilde{\chi}_M^H(\gamma) = \min_{n \in \mathbb{N}} \tilde{\chi}_n^H(\gamma)$ for a fixed $\gamma > 0$.*

One can find the proof for Lemma 3.3 in Appendix B. Similarly to Lemma 2.4, we can also prove the properties of eigenvalues of (3.3) as follows.

LEMMA 3.4. *For a fixed $\gamma > 0$, let $\tilde{\chi}_n^S(\gamma)$, $\tilde{\chi}_n^H(\gamma)$, $\tilde{\chi}_\infty^S(\gamma)$ be defined as in (3.4), (3.5), (3.7), and $\tilde{\chi}_N^S(\gamma)$, $\tilde{\chi}_M^H(\gamma)$ in Lemma 3.3. We further define*

$$(3.8) \quad \chi^-(\gamma) = \tilde{\chi}_N^S(\gamma), \quad \chi^+(\gamma) = \min \{ \tilde{\chi}_M^H(\gamma), \tilde{\chi}_\infty^S(\gamma) \}.$$

Then we have the following results:

- (i) When $\chi^-(\gamma) < \chi < \chi^+(\gamma)$, all the eigenvalues of (3.3) have negative real parts.
- (ii) When $\chi \geq \chi^+(\gamma)$, $\mu = \pm i\omega_n$ ($\omega_n > 0$) is a pair of purely imaginary roots of (2.6) if $\chi = \tilde{\chi}_n^H(\gamma)$.
- (iii) When $\chi \leq \chi^-(\gamma)$ or $\chi \geq \chi^+(\gamma)$, $\mu = 0$ is a root of (2.6) if $\chi = \tilde{\chi}_n^S(\gamma)$.

Remark 3.5. The boundary curve $\chi = \chi^+(\gamma)$ for the constant steady state of system (1.4) to lose stability consists of two types of bifurcation curve $\chi = \tilde{\chi}_M^H(\gamma)$ and $\chi = \tilde{\chi}_\infty^S(\gamma)$. When the constant steady state loses its stability via $\chi = \tilde{\chi}_\infty^S(\gamma)$, there will be infinitely many eigenvalues with positive real parts for the corresponding linearized system. This situation also happens in an explicit spatial memory model studied in [27].

Similarly to Lemma 2.5, we can verify that the following transversality condition for Hopf bifurcation holds in system (1.4) and we omit the proof.

LEMMA 3.6. Let $\chi = \tilde{\chi}_n^H(\gamma)$ be defined as in (3.5). Then (3.3) has a pair of roots in the form $\mu = \eta(\chi) \pm i\omega(\chi)$ when χ is near $\tilde{\chi}_n^H(\gamma)$ such that $\eta(\tilde{\chi}_n^H(\gamma)) = 0$ and $\eta'(\tilde{\chi}_n^H(\gamma)) > 0$.

By Lemmas 3.3, 3.4, and 3.6 and Hopf bifurcation theory for partial functional differential equations, we obtain the following results on the stability and bifurcation behaviors of the positive homogeneous steady state of (1.4).

THEOREM 3.7. Assume that the conditions in (A) hold, and let $\tilde{\chi}_n^S(\gamma)$, $\tilde{\chi}_n^H(\gamma)$ be defined as in (3.4), (3.5), and $\chi^-(\gamma)$, $\chi^+(\gamma)$ in (3.8). We have the following results for (1.4):

- (i) A mode- n Turing bifurcation occurs at $\chi = \tilde{\chi}_n^S(\gamma)$ for $\gamma > 0$ and $n \in \mathbb{N}$, and thus a mode- n spatially nonhomogeneous steady state can arise near $(\theta, v_\theta, \tilde{q}_\theta)$.
- (ii) A mode- n Hopf bifurcation occurs at $\chi = \tilde{\chi}_n^H(\gamma)$ for $\gamma > 0$ and $n \in \mathbb{N}$, and the bifurcating periodic solutions are spatially nonhomogeneous.
- (iii) If we fix $\gamma \in (0, +\infty)$, the positive homogeneous steady state $(\theta, v_\theta, \tilde{q}_\theta)$ is locally asymptotically stable for $\chi^-(\gamma) < \chi < \chi^+(\gamma)$ and unstable for $\chi \in (-\infty, \chi^-(\gamma)) \cup (\chi^+(\gamma), +\infty)$.

Fixing the parameters as $d_1 = 0.01$, $d_2 = 0.02$, $m = 0.5$, $d = 0.1$, $k = 1$, $b = 0.2$, $\xi = 0.3$, the bifurcation diagram of (1.4) is illustrated in Figure 4. We see that the dynamics of (1.4) is different from that of (1.3): (i) there exists a limiting Turing curve $\chi = \tilde{\chi}_\infty^S(\gamma)$ corresponding to the infinite mode which destabilizes the system when $\chi > \tilde{\chi}_\infty^S(\gamma)$; (ii) different modes of Hopf bifurcation curves can intersect with each other such that codimension-2 double Hopf bifurcation occurs. Near the intersection point of mode-3 and mode-4 Hopf bifurcation curves, we choose proper parameter values as presented in P2, P3, and P4 to perform simulations. When the parameters are taken as $(\chi, \gamma) = P2$, which is extremely close to the mode-4 Hopf bifurcation curve, we observe that a mode-4 spatially nonhomogeneous periodic pattern arises, as shown in Figure 5(b). When $(\chi, \gamma) = P3$, which is in between the area enclosed by the two Hopf bifurcation curves and $(\chi, \gamma) = P4$, which is closest to the mode-3 Hopf bifurcation curve, we observe a quasi-periodic pattern and a mode-3 periodic pattern, respectively, as illustrated in Figures 5(c) and (d). Compared to the periodic patterns observed in system (1.3) (see Figure 2), the spatial distribution of resources is more diverse, and even quasi-periodic distribution is possible due to the impact of the consumption process on cognition and memory in system (1.4).

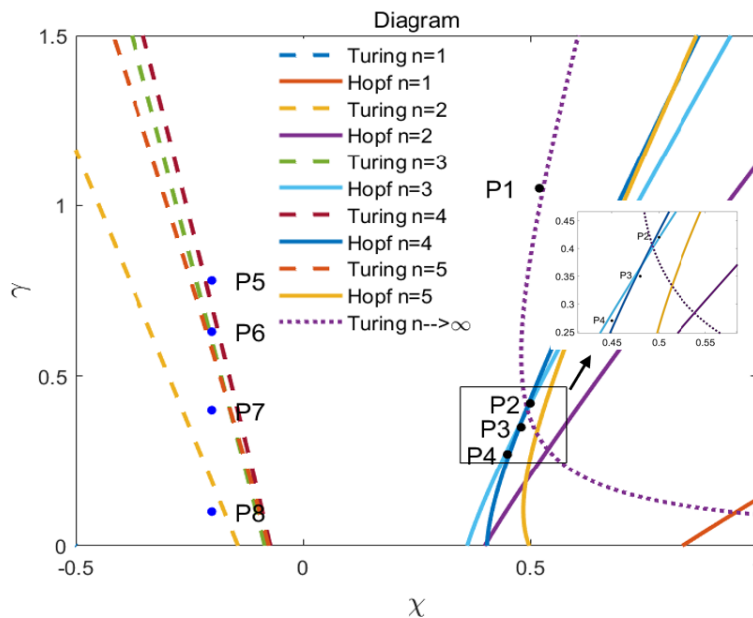


FIG. 4. The bifurcation diagram of system (1.4) in parameter plane (χ, γ) with $d_1 = 0.01$, $d_2 = 0.02$, $m = 0.5$, $d = 0.1$, $k = 1$, $b = 0.2$, $\xi = 0.3$, $\Omega = (0, \pi)$, and the Turing bifurcation curves $\chi = \tilde{\chi}_n^S(\gamma)$ defined as in (3.4) can be identified by the dashed curves and the Hopf bifurcation curves $\chi = \tilde{\chi}_n^H(\gamma)$ defined as in (3.5) by the solid curves. In addition, the dotted curve denotes the limiting Turing curve $\chi = \tilde{\chi}_\infty^S(\gamma)$ defined as in (3.7). The parameter values for the numerical simulations are P1 (0.52, 1.05), P2 (0.50, 0.42), P3 (0.48, 0.35), P4 (0.45, 0.27), P5 (-0.2, 0.78), P6 (-0.2, 0.63), P7 (-0.2, 0.40), and P8 (-0.2, 0.10).

In Figure 6, we illustrate the spatially nonhomogeneous steady state and some wandering periodic patterns when $\chi = -0.2$. When we choose $\gamma = 0.78$ corresponding to P5 in Figure 4, the constant steady state $(\theta, v_\theta, \bar{q}_\theta)$ is stable, as shown in (a). If we decrease γ to 0.63 corresponding to P5, which is under the mode-4 Turing curve, a mode-4 spatially nonhomogeneous steady state arises, as shown in (b). When we continue to decrease the γ value to 0.40, the mode-4 steady state is still stable, as shown in (c). Similarly to model (1.3), we observe a “wandering” pattern with a large period for $\gamma = 0.10$, as shown in (d).

4. Discussion. In [41], Wang and Salmaniw summarized three main categories of cognitive processes in animal movement models: perception, memory, and learning. Perception means the ability to see, hear, or otherwise become aware of something through the senses, while memory is the ability to store, retain, and retrieve information [6, 11]. Learning is the information acquisition from an individual experience [11]. Spatial memory modeled by explicit time delay has received much attention: (i) discrete delay [2, 13, 25, 26, 27, 30, 31, 32, 34, 40, 42, 43, 44, 46]; (ii) distributed delay [15, 24, 28, 35, 47]; (iii) nonlocal delay [29].

Through these studies, we can gain some insight into the effect of explicit memory in delayed form on animal movement. However, there is little analysis completed for implicit memory that is described by a learning equation [33, 41]. In this paper, we consider resource-consumer models with implicit spatial memory by incorporating an additional biased diffusion term which shows an attractive movement of consumers to

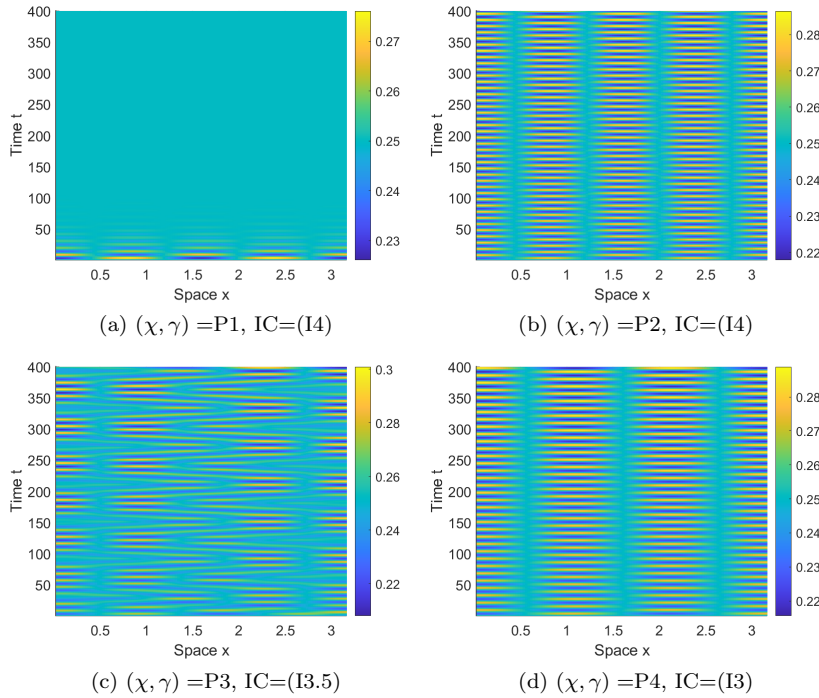


FIG. 5. Periodic patterns arising near Hopf bifurcation curves in system (1.4) when parameters are $d_1 = 0.01$, $d_2 = 0.02$, $m = 0.5$, $d = 0.1$, $k = 1$, $b = 0.2$, $\xi = 0.3$, and $\Omega = (0, \pi)$. In each figure, the color indicates the value of $u(x, t)$ according to the color bar.

the resource. The difference between these two models lies in the cognitive potential function $q(x, t)$ satisfying two different learning ODEs. System (1.3)/(1.4) is a PDE-ODE coupled system whose linearized system has a more complicated spectrum than a classical reaction-diffusion system. We first perform a spectral analysis for each system and found that the spectral set of the corresponding linear system for (1.3)/(1.4) is discrete, which implies that the stability of the constant steady state is still determined by the corresponding eigenvalue problem. Next, we take the perceptual diffusion rate $\chi \in \mathbb{R}$ as a bifurcation parameter and perform a bifurcation analysis for system (1.3)/(1.4).

In systems (1.3) and (1.4), steady-state bifurcation and Hopf bifurcation can both occur. From the bifurcation diagram in Figures 1 and 4, we observe that the constant steady states are stable for a small perceptual diffusion rate (either attractive or repulsive), while a large perceptual diffusion can destabilize the systems and induce rich spatial patterns. The outcome differences between these two models mainly lie in the following two aspects:

1. All the steady-state bifurcation curves lie in the left half part of the $\chi-\gamma$ plane in system (1.3). In system (1.4), there exists an n_* defined as in Lemma 3.3 such that the steady-state bifurcation curves move to the right half plane when $n \geq n_*$. In particular, when $n \rightarrow +\infty$, we found a limiting Turing curve $\chi = \tilde{\chi}_\infty^S$ such that the linearized system at the constant steady state has infinitely many eigenvalues with positive real parts for $\chi > \tilde{\chi}_\infty^S$.

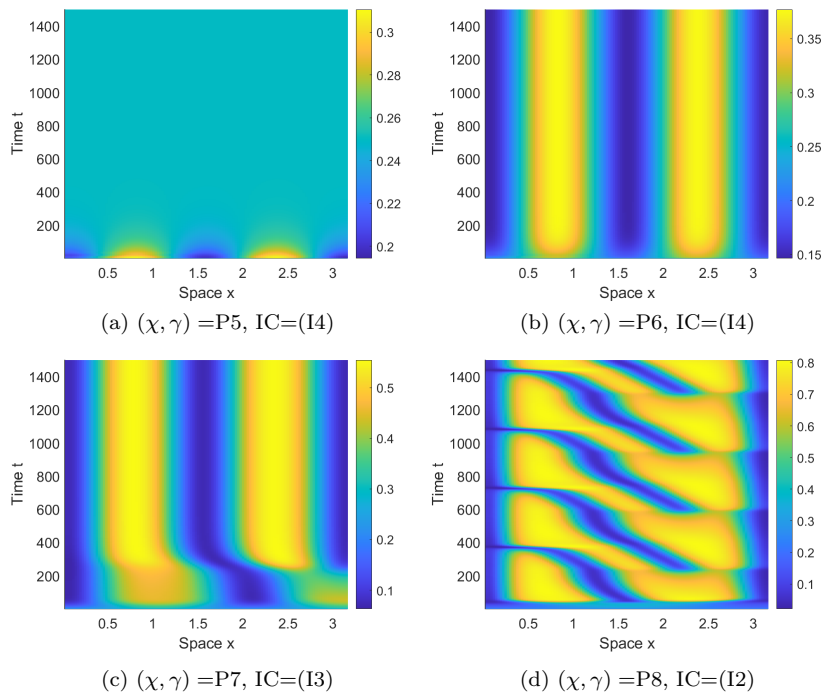


FIG. 6. Spatially nonhomogeneous steady state arising near Turing bifurcation curves in system (1.4) when parameters are $d_1 = 0.01$, $d_2 = 0.02$, $m = 0.5$, $d = 0.1$, $k = 1$, $b = 0.2$, $\xi = 0.3$, and $\Omega = (0, \pi)$. In each figure, the color indicates the value of $u(x, t)$ according to the color bar.

2. In system (1.3), the dominant mode for Hopf bifurcation will not vary with different perceptual diffusion rates when the other parameters are fixed. For example, we observed that the mode-2 Hopf bifurcation is stable when the parameter values are taken as in Figure 1. However, it is shown that there are different dominant modes for different perceptual diffusion rates in system (1.4), even two different modes of Hopf bifurcation curve can intersect with each other such that a codimension-2 double Hopf bifurcation occurs; see Figure 4 and 5.

Based on the above theoretical reasons, the dynamics of system (1.4) are richer; for instance, different modes of stable periodic patterns and quasi-periodic patterns can be found in system (1.4). From a biological perspective, these results indicate that the distribution of the resources/consumers seems to be more spatially diverse when the cognitive map $q(x, t)$ follows the more realistic learning equation (H2).

This paper considered local perception when the cognitive kernel $g(x)$ is a delta function, which is the limiting case when the perceptual range is extremely narrow. However, the actual situation is that the animal has a restricted habitat and wide perceptual range, and thus it is more realistic when the kernel function is taken as a top-hat, Gaussian, or exponential form. Therefore, we will consider the effect of nonlocal perception in consumer-resource models in the future.

Appendix A. The proof of Theorem 3.1. In order to analyze the spectrum of \mathcal{L} defined as in (2.4), we consider the nonhomogeneous problem

$$(A.1) \quad \begin{cases} d_1 \Delta \phi + \beta \phi - d\psi = \mu \phi + \tau_1, \\ d_2 \Delta \psi - \chi v_\theta \Delta \phi + \alpha \phi = \mu \psi + \tau_2, \\ bv_\theta \phi + \frac{b\theta\gamma}{\gamma + \xi v_\theta} \psi - \gamma \varphi = \mu \varphi + \tau_3, \\ \partial_\nu \phi = \partial_\nu \psi = 0, \end{cases}$$

where $\mu \in \mathbb{C}$ and $(\tau_1, \tau_2, \tau_3) \in Y$. There are the following two cases according to the solution of the third equation in (A.1).

Case 1: $\mu \neq -\gamma - \xi v_\theta$. From the third equation of (A.1), we can obtain $\varphi = bv_\theta \phi + \frac{b\theta\gamma}{\gamma + \xi v_\theta} \psi - \tau_3$ and, substituting it into the second equation, we have

$$(A.2) \quad \begin{cases} d_1 \Delta \phi + \beta \phi - d\psi = \mu \phi + \tau_1, \\ d_2 \Delta \psi - \frac{\chi v_\theta}{\mu + \gamma + \xi v_\theta} \Delta \left(bv_\theta \phi + \frac{b\theta\gamma}{\gamma + \xi v_\theta} \psi - \tau_3 \right) + \alpha \phi = \mu \psi + \tau_2, \\ \partial_\nu \phi = \partial_\nu \psi = 0, \end{cases}$$

which is equivalent to

$$\tilde{\mathcal{L}}_1 \begin{pmatrix} \phi \\ \psi \end{pmatrix} = \begin{pmatrix} d_1 \Delta \phi + \beta \phi - d\psi - \mu \phi \\ d_2 \Delta \psi - \frac{b\chi v_\theta}{\mu + \gamma + \xi v_\theta} \Delta \phi + \alpha \phi - \mu \psi \end{pmatrix} = \begin{pmatrix} \tau_1 \\ \tau_2 - \frac{\chi v_\theta}{\mu + \gamma} \Delta \tau_3 \end{pmatrix}.$$

By an argument similar to that in the proof of Theorem 2.1, we know that $\tilde{\mathcal{L}}_1$ has a bounded inverse $\tilde{\mathcal{L}}_1^{-1}$ with

$$\begin{aligned} & \|\phi\|_{W_N^{2,p}(\Omega)} + \|\psi\|_{W_N^{2,p}(\Omega)} \\ & \leq \|\tilde{\mathcal{L}}_1^{-1}\| \left(\|d_1 \Delta \phi + \beta \phi - d\psi\|_{L^p(\Omega)} + \left\| d_2 \Delta \psi - \frac{b\chi v_\theta}{\mu + \gamma + \xi v_\theta} \Delta \phi + \alpha \phi \right\|_{L^p(\Omega)} \right), \end{aligned}$$

when $\mu \in \mathbb{C}$ satisfies the inequality

$$(A.3) \quad \begin{aligned} & (\mu + d_1 \lambda_n - \beta)(\mu + \gamma + \xi v_\theta)[(\mu + d_2 \lambda_n)(\gamma + \xi v_\theta) - \xi v_\theta b \theta \gamma] + d\alpha(\mu + \gamma + \xi v_\theta) \\ & + db\chi v_\theta^2 \lambda_n \neq 0. \end{aligned}$$

Therefore, we know that $\tilde{\mathcal{L}} - (\mu + \xi v_\theta)I$ has a bounded inverse $(\tilde{\mathcal{L}} - (\mu + \xi v_\theta)I)^{-1}$.

If (A.3) does not hold, then it can be inferred that μ satisfies the dispersal relation (3.3), which has three roots $\tilde{\mu}_n^{(j)}$, $j = 1, 2, 3$, for each $n \in \mathbb{N}_0$. For $j = 1, 2, 3$, we put $\mu = \tilde{\mu}_n^{(j)}$ into (A.1), and one can check that $\tilde{\mu}_n^{(j)}$ are indeed eigenvalues of $\tilde{\mathcal{L}}$ with eigenfunctions being

$$\begin{pmatrix} \tilde{\phi}_n^{(j)} \\ \tilde{\psi}_n^{(j)} \\ \tilde{\varphi}_n^{(j)} \end{pmatrix} = \begin{pmatrix} 1 \\ \frac{1}{d}(-d_1 \lambda_n + \beta - \tilde{\mu}_n^{(j)}) \\ \frac{dbv_\theta(\gamma + \xi v_\theta) - b\theta\gamma(d_1 \lambda_n + \tilde{\mu}_n^{(j)} - \beta)}{(\tilde{\mu}_n^{(j)} + \gamma + \xi v_\theta)(\gamma + \xi v_\theta)} \end{pmatrix} \phi_n,$$

which implies that $Ker(\tilde{\mathcal{L}} - \tilde{\mu}_n^{(j)}) = Span\{\tilde{\phi}_n^{(j)}, \tilde{\psi}_n^{(j)}, \tilde{\varphi}_n^{(j)}\}^T$.

Case 2: $\mu = -\gamma - \xi v_\theta$. In this case, (A.1) can be solved as

$$\begin{cases} d_1 \Delta \phi + \left(\beta - \gamma - \xi v_\theta + \frac{bdv_\theta(\gamma + \xi v_\theta)}{b\theta\gamma} \right) \phi = \tau_1 + \frac{d(\gamma + \xi v_\theta)\tau_3}{b\theta\gamma}, \\ \psi = \frac{(\gamma + \xi v_\theta)(\tau_3 - bv_\theta\phi)}{b\theta\gamma}, \\ \Delta \varphi = \frac{1}{\chi v_\theta} (d_2 \Delta \psi + \alpha \phi - (\gamma + \xi v_\theta)\psi - \tau_2). \end{cases}$$

By letting $\tau_1 = \tau_2 = \tau_3 = 0$, we know that the first equation only has trivial solution $\phi = 0$ when $\beta - \gamma - \xi v_\theta + \frac{bdv_\theta(\gamma + \xi v_\theta)}{b\theta\gamma} \notin \{\lambda_n\}_{n=1}^\infty$. Also, we have $\psi = 0$ from the second equation and $\Delta \varphi = 0$, which implies that $\text{Ker}(\tilde{\mathcal{L}} + (\gamma + \xi v_\theta)I) = \text{Span}\{(0, 0, \tilde{\varphi})^T\}$ with $\Delta \tilde{\varphi} = 0$ and thus $-\gamma - \xi v_\theta \in \sigma_p(\tilde{\mathcal{L}})$. If $\beta - \gamma - \xi v_\theta + \frac{bdv_\theta(\gamma + \xi v_\theta)}{b\theta\gamma} = \lambda_n$ holds for some $n \in \mathbb{N}$, then we have

$$\begin{aligned} \phi &= \tilde{\phi}_n = d_1 \phi_n, \quad \psi = \tilde{\psi}_n = -\frac{d_1 v_\theta(\gamma + \xi v_\theta)\phi_n}{\theta\gamma}, \\ \varphi &= \tilde{\varphi}_n = \frac{1}{\chi\theta v_\theta} d_1 d_2 v_\theta (\gamma + \xi v_\theta \lambda_n + \alpha d_1 \theta \gamma + d_1 v_\theta (\gamma + \xi v_\theta)^2) \phi_n. \end{aligned}$$

Still, we have $-\gamma - \xi v_\theta \in \sigma_p(\tilde{\mathcal{L}})$ with $\text{Ker}(\tilde{\mathcal{L}} + (\gamma + \xi v_\theta)I) = \text{Span}\{(\tilde{\phi}_n, \tilde{\psi}_n, \tilde{\varphi}_n)^T\}$. This completes the proof.

Appendix B. The proof of Lemma 3.3. By the definition of $\tilde{\chi}_n^S(\gamma)$ given in (3.4), we see that $\tilde{\chi}_n^S(\gamma) = Q_n(\gamma)/P_n(\gamma)$ with $Q_n(\gamma)$ and $P_n(\gamma)$ defined as in (3.6). It can be verified that $Q_n(\gamma) > 0$ for all $\gamma > 0$, and therefore the sign of $\tilde{\chi}_n^S(\gamma)$ is determined by the sign of $P_n(\gamma)$. By letting $P_n(\gamma) > 0$, we have

$$(B.1) \quad \lambda_n < \frac{dv_\theta(\gamma + \xi v_\theta)}{d_1 \gamma \theta} \in \left(\frac{dv_\theta}{d_1 \theta}, +\infty \right),$$

which implies that $P_n(\gamma) > 0$ holds for all $\gamma > 0$ when $\lambda_n < \frac{dv_\theta}{d_1 \theta}$, and $n_* \in \mathbb{N}$ is the largest integer such that $\lambda_{n_*} < \frac{dv_\theta}{d_1 \theta}$. When $n \leq n_*$, $\tilde{\chi}_n^S(\gamma) < 0$ holds for all $\gamma > 0$. When $n > n_*$, we have

$$P_n(0) = bdv_\theta^2 \lambda_n > 0, \quad \lim_{\gamma \rightarrow +\infty} P_n(\gamma) = -(d_1 \lambda_n - \beta)b\theta v_\theta \lambda_n < 0,$$

and

$$\frac{d[P_n(\gamma)]}{d\gamma} = -\frac{(d_1 \lambda_n - \beta)b\theta \xi \lambda_n v_\theta^2}{(\gamma + \xi v_\theta)^2} < 0,$$

and thus there exists $\gamma_n^* > 0$ such that $P_n(\gamma_n^*) = 0$, and $P_n(\gamma) > 0$ for $\gamma \in (0, \gamma_n^*)$ and $P_n(\gamma) < 0$ for $\gamma \in (\gamma_n^*, +\infty)$.

Then we determine the monotonicity of $\tilde{\chi}_n^S(\gamma)$ concerning n and rewrite $\tilde{\chi}_n^S(\gamma)$ in the following form by letting $p = \lambda_n$:

$$\tilde{\chi}_p^S(\gamma) = -\frac{(\gamma + \xi v_\theta)(d_2 p(d_1 p - \beta) + d\alpha)}{bdv_\theta^2 p - (d_1 p - \beta) \frac{b\theta \gamma v_\theta p}{\gamma + \xi v_\theta}}.$$

Taking the derivative with respect to p , we have

$$\frac{d[\tilde{\chi}_p^S(\gamma)]}{dp} = -\frac{\gamma + \xi v_\theta}{P_n^2(\gamma)} \left[d_1 d_2 b d v_\theta^2 p^2 + \frac{2d\alpha d_1 b \theta \gamma v_\theta}{(\gamma + \xi v_\theta)} p - \frac{d\alpha (bdv_\theta^2(\gamma + \xi v_\theta) + \beta b\theta \gamma v_\theta)}{(\gamma + \xi v_\theta)} \right].$$

From the expression of $\frac{d[\tilde{\chi}_p^S(\gamma)]}{dp}$, we see that $\frac{d[\tilde{\chi}_p^S(\gamma)]}{dp}$ is a quadratic function of p with positive coefficients for quadratic and linear terms. However, the constant term is negative as $b\delta v_\theta^2(\gamma + \xi v_\theta) + \beta b\theta\gamma v_\theta > 0$ when $\tilde{\chi}_n^S(\gamma) > 0$, which implies that $\frac{d[\tilde{\chi}_p^S(\gamma)]}{dp}$ has a unique zero p^* such that $\frac{d[\tilde{\chi}_p^S(\gamma)]}{dp} > 0$ for $p \in (0, p^*)$ and $\frac{d[\tilde{\chi}_p^S(\gamma)]}{dp} < 0$ for $p \in (p^*, +\infty)$ and $\tilde{\chi}_p^S(\gamma)$ reaches its maximum at p^* . Let $N \in \mathbb{N}$ be the integer such that λ_n is the closest eigenvalue to p^* . Then we have $\tilde{\chi}_N^S(\gamma) = \max_{n \in \mathbb{N}} \tilde{\chi}_n^S(\gamma)$ for a fixed $\gamma > 0$. This proves (i)-a.

When $\tilde{\chi}_n^S(\gamma) > 0$, the constant term in the expression of $\frac{d[\tilde{\chi}_p^S(\gamma)]}{dp}$ is positive, and thus we know that $\frac{d[\tilde{\chi}_p^S(\gamma)]}{dp} < 0$ from the discussion in the proof of (i)-a. Therefore, $\tilde{\chi}_n^S(\gamma)$ is strictly decreasing with respect to n and we have

$$(B.2) \quad \min_{n > n_*} \tilde{\chi}_n^S(\gamma) = \lim_{n \rightarrow +\infty} \tilde{\chi}_n^S(\gamma) = \frac{d_2(\gamma + \xi v_\theta^2)}{b\theta\gamma v_\theta}.$$

Define the limiting Turing curve as $\tilde{\chi}_\infty^S$ in (3.7) by letting $\lambda_n \rightarrow +\infty$ in (3.4), and it can be known that $\tilde{\chi}_\infty^S(\gamma)$ is first a decreasing and then increasing function of γ and reaches its minimum at $\gamma = \gamma_*$. This proves the conclusions in (i)-b.

To prove (ii), we rewrite $\tilde{\chi}_n^H(\gamma)$ as

$$\begin{aligned} \tilde{\chi}_p^H(\gamma) = & \frac{((d_1 + d_2)p - \beta)}{bdv_\theta^2 p + b\theta\gamma v_\theta p + \frac{d_2 b\theta\gamma v_\theta p^2}{\gamma + \xi v_\theta}} [d_2 p(d_1 p - \beta) \\ & + (\gamma + \xi v_\theta)((d_1 + d_2)p - \beta) + (\gamma + \xi v_\theta)^2 + d\alpha], \end{aligned}$$

where λ_n in $\tilde{\chi}_n^H(\gamma)$ is replaced by p . Taking the derivative with respect to p , we obtain

$$\frac{d[\tilde{\chi}_p^H(\gamma)]}{dp} = \frac{F_p(\gamma)}{H_p^2(\gamma)},$$

where

$$\begin{aligned} F_p(\gamma) = & H_p(\gamma) \{ (d_1 + d_2) [d_2 p(d_1 p - \beta) + (\gamma + \xi v_\theta)((d_1 + d_2)p - \beta) + (\gamma + \xi v_\theta)^2 \\ & + d\alpha] + ((d_1 + d_2)p - \beta)(2d_1 d_2 p - \beta + (d_1 + d_2)(\gamma + \xi v_\theta)) \} \\ & - Q_p(\gamma) \left(b\delta v_\theta^2 + b\theta\gamma v_\theta + \frac{2d_2 b\theta\gamma v_\theta p}{\gamma + \xi v_\theta} \right) \end{aligned}$$

and

$$\begin{aligned} Q_p(\gamma) = & ((d_1 + d_2)p - \beta) [d_2 p(d_1 p - \beta) + (\gamma + \xi v_\theta)((d_1 + d_2)p - \beta) \\ & + (\gamma + \xi v_\theta)^2 + d\alpha], \\ H_p(\gamma) = & b\delta v_\theta^2 p + b\theta\gamma v_\theta p + \frac{d_2 b\theta\gamma v_\theta p^2}{\gamma + \xi v_\theta}. \end{aligned}$$

By a tedious calculation, one can verify that $F_p(\gamma)$ is a quartic polynomial of p , that is,

$$F_p(\gamma) = a_4(\gamma)p^4 + a_3(\gamma)p^3 + a_2(\gamma)p^2 + a_1(\gamma)p + a_0(\gamma),$$

with

$$\begin{aligned} a_4(\gamma) = & \frac{(d_1 + d_2)d_1 d_2^2 b\theta\gamma v_\theta}{\gamma + \xi v_\theta} > 0, \\ a_0(\gamma) = & \beta(b\delta v_\theta^2 + b\theta\gamma v_\theta)[\alpha + (\gamma + \xi v_\theta)^2 - \beta(\gamma + \xi v_\theta)] < 0. \end{aligned}$$

Therefore, it can be inferred that there exists at least one positive zero $p = p^{**}$ of $F_p(\gamma)$ such that $\tilde{\chi}_p^H(\gamma)$ reaches its minimum at $p = p^{**}$. Therefore, we may take $M \in \mathbb{N}$ such that λ_M is the closest eigenvalue to p^{**} . This completes the proof.

Acknowledgments. We would like to thank the editor and two anonymous referees for helpful comments and suggestions on our manuscript, which significantly improved the quality of our paper.

REFERENCES

- [1] B. ABRAHMS, E. L. HAZEN, E. O. AIKENS, M. S. SAVOCA, J. A. GOLDBOGEN, S. J. BOGRAD, M. G. JACOX, L. M. IRVINE, D. M. PALACIOS, AND B. R. MATE, *Memory and resource tracking drive blue whale migrations*, Proc. Natl. Acad. Sci. USA, 116 (2019), pp. 5582–5587.
- [2] Q. AN, C. C. WANG, AND H. WANG, *Analysis of a spatial memory model with nonlocal maturation delay and hostile boundary condition*, Discrete Contin. Dyn. Syst., 40 (2020), pp. 5845–5868, <https://doi.org/10.3934/dcds.2020249>.
- [3] S. S. CHEN, J. P. SHI, AND G. H. ZHANG, *Spatial pattern formation in activator-inhibitor models with nonlocal dispersal*, Discrete Contin. Dyn. Syst. Ser. B, 26 (2021), pp. 1843–1866, <https://doi.org/10.3934/dcdsb.2020042>.
- [4] W. F. FAGAN, *Migrating whales depend on memory to exploit reliable resources*, Proc. Natl. Acad. Sci. USA, 116 (2019), pp. 5217–5219.
- [5] W. F. FAGAN, E. GURARIE, S. BEWICK, A. HOWARD, R. S. CANTRELL, AND C. COSNER, *Perceptual ranges, information gathering, and foraging success in dynamic landscapes*, Amer. Nat., 189 (2017), pp. 474–489.
- [6] W. F. FAGAN, M. A. LEWIS, M. AUGER-MÉTHÉ, T. AVGAR, S. BENHAMOU, G. BREED, L. LADAGE, U. E. SCHLÄGEL, W. W. TANG, Y. P. PAPASTAMATIOU, J. FORESTER, AND T. MUELLER, *Spatial memory and animal movement*, Ecol. Lett., 16 (2013), pp. 1316–1329.
- [7] M. B. FENTON, *Bats navigate with cognitive maps*, Science, 369 (2020), pp. 142–142.
- [8] A. P. FOSS-GRANT, *Quantitative Challenges in Ecology: Competition, Migration, and Social Learning*, Ph.D. thesis, University of Maryland, 2017.
- [9] R. GOLLEDGE, *Wayfinding Behavior: Cognitive Mapping and Other Spatial Processes*, Johns Hopkins University Press, 1998.
- [10] D. HENRY, *Geometric Theory of Semilinear Parabolic Equations [Electronic Resource]*, Springer, New York, 1981.
- [11] M. A. LEWIS, W. F. FAGAN, M. AUGER-MÉTHÉ, J. FRAIR, J. M. FRYXELL, C. GROS, E. GURARIE, S. D. HEALY, AND J. A. MERKLE, *Learning and animal movement*, Front. Ecol. Evol., 9 (2021), 681704.
- [12] M. A. LEWIS AND J. D. MURRAY, *Modelling territoriality and wolf–deer interactions*, Nature, 366 (1993), pp. 738–740.
- [13] S. LI, S. L. YUAN, Z. JIN, AND H. WANG, *Bifurcation analysis in a diffusive predator-prey model with spatial memory of prey, Allee effect and maturation delay of predator*, J. Differential Equations, 357 (2023), pp. 32–63, <https://doi.org/10.1016/j.jde.2023.02.009>.
- [14] Y. LI, A. MARCINIAK-CZOCHRA, I. TAKAGI, AND B. Y. WU, *Bifurcation analysis of a diffusion-ODE model with Turing instability and hysteresis*, Hiroshima Math. J., 47 (2017), pp. 217–247, <https://doi.org/10.32917/hmj/1499392826>.
- [15] J. LIN AND Y. L. SONG, *Spatially inhomogeneous periodic patterns induced by distributed memory in the memory-based single population model*, Appl. Math. Lett., 137 (2023), 108490, <https://doi.org/10.1016/j.aml.2022.108490>.
- [16] A. MARCINIAK-CZOCHRA, G. KARCH, AND K. SUZUKI, *Instability of Turing patterns in reaction-diffusion-ODE systems*, J. Math. Biol., 74 (2017), pp. 583–618, <https://doi.org/10.1007/s00285-016-1035-z>.
- [17] P. R. MOORCROFT AND M. A. LEWIS, *Mechanistic Home Range Analysis*, Princeton University Press, 2006.
- [18] P. R. MOORCROFT, M. A. LEWIS, AND R. L. CRABTREE, *Home range analysis using a mechanistic home range model*, Ecology, 80 (1999), pp. 1656–1665.
- [19] J. O’KEEFE AND L. NADEL, *The Hippocampus as a Cognitive Map*, Oxford University Press, 1978.
- [20] K. J. PAINTER AND T. HILLEN, *Spatio-temporal chaos in a chemotaxis model*, Phys. D, 240 (2011), pp. 363–375.
- [21] J. R. POTTS AND M. A. LEWIS, *How memory of direct animal interactions can lead to territorial pattern formation*, J. R. Soc. Interface, 13 (2016), 20160059.

- [22] J. R. POTTS AND M. A. LEWIS, *Spatial memory and taxis-driven pattern formation in model ecosystems*, Bull. Math. Biol., 81 (2019), pp. 2725–2747.
- [23] U. E. SCHLÄGEL AND M. A. LEWIS, *Detecting effects of spatial memory and dynamic information on animal movement decisions*, Methods Ecol. Evol., 5 (2014), pp. 1236–1246.
- [24] H. SHEN, Y. L. SONG, AND H. WANG, *Bifurcations in a diffusive resource-consumer model with distributed memory*, J. Differential Equations, 347 (2023), pp. 170–211, <https://doi.org/10.1016/j.jde.2022.11.044>.
- [25] J. P. SHI, C. C. WANG, AND H. WANG, *Diffusive spatial movement with memory and maturation delays*, Nonlinearity, 32 (2019), pp. 3188–3208.
- [26] J. P. SHI, C. C. WANG, AND H. WANG, *Spatial movement with diffusion and memory-based self-diffusion and cross-diffusion*, J. Differential Equations, 305 (2021), pp. 242–269, <https://doi.org/10.1016/j.jde.2021.10.021>.
- [27] J. P. SHI, C. C. WANG, H. WANG, AND X. P. YAN, *Diffusive spatial movement with memory*, J. Dynam. Differential Equations, 32 (2020), pp. 979–1002.
- [28] Q. Y. SHI, J. P. SHI, AND H. WANG, *Spatial movement with distributed memory*, J. Math. Biol., 82 (2021), 33, <https://doi.org/10.1007/s00285-021-01588-0>.
- [29] Q. Y. SHI AND Y. L. SONG, *Spatial movement with nonlocal memory*, Discrete Contin. Dyn. Syst. Ser. B, 28 (2023), pp. 5580–5596, <https://doi.org/10.3934/dcdsb.2023067>.
- [30] Y. L. SONG, Y. H. PENG, AND T. H. ZHANG, *The spatially inhomogeneous Hopf bifurcation induced by memory delay in a memory-based diffusion system*, J. Differential Equations, 300 (2021), pp. 597–624, <https://doi.org/10.1016/j.jde.2021.08.010>.
- [31] Y. L. SONG, Y. H. PENG, AND T. H. ZHANG, *Double Hopf bifurcation analysis in the memory-based diffusion system*, J. Dynam. Differential Equations, (2022), <https://doi.org/10.1007/s10884-022-10180-z>.
- [32] Y. L. SONG, J. P. SHI, AND H. WANG, *Spatiotemporal dynamics of a diffusive consumer-resource model with explicit spatial memory*, Stud. Appl. Math., 148 (2022), pp. 373–395, <https://doi.org/10.1111/sapm.12443>.
- [33] Y. L. SONG, H. WANG, AND J. F. WANG, *Cognitive consumer-resource spatiotemporal dynamics with nonlocal perception*, J. Nonlinear Sci., 34 (2024), 19, <https://doi.org/10.1007/s00332-023-09996-w>.
- [34] Y. L. SONG, S. H. WU, AND H. WANG, *Spatiotemporal dynamics in the single population model with memory-based diffusion and nonlocal effect*, J. Differential Equations, 267 (2019), pp. 6316–6351, <https://doi.org/10.1016/j.jde.2019.06.025>.
- [35] Y. L. SONG, S. H. WU, AND H. WANG, *Memory-based movement with spatiotemporal distributed delays in diffusion and reaction*, Appl. Math. Comput., 404 (2021), 126254, <https://doi.org/10.1016/j.amc.2021.126254>.
- [36] C. S. TEITELBAUM, S. J. CONVERSE, W. F. FAGAN, K. BÖHNING-GAESE, R. B. O’HARA, A. E. LACY, AND T. MUELLER, *Experience drives innovation of new migration patterns of whooping cranes in response to global change*, Nat. Commun., 7 (2016), 12793.
- [37] S. TOLEDO, D. SHOHAMI, I. SCHIFFNER, E. LOURIE, Y. ORCHAN, Y. BARTAN, AND R. NATHAN, *Cognitive map-based navigation in wild bats revealed by a new high-throughput tracking system*, Science, 369 (2020), pp. 188–193.
- [38] A. M. TURING, *The chemical basis of morphogenesis*, Philos. Trans. Roy. Soc. London Ser. B, 237 (1952), pp. 37–72.
- [39] J. VAN NEERVEN, *Functional Analysis*, Cambridge University Press, 2022.
- [40] C. H. WANG, S. L. YUAN, AND H. WANG, *Spatiotemporal patterns of a diffusive prey-predator model with spatial memory and pregnancy period in an intimidatory environment*, J. Math. Biol., 84 (2022), 12, <https://doi.org/10.1007/s00285-022-01716-4>.
- [41] H. WANG AND Y. SALMANIW, *Open problems in PDE models for knowledge-based animal movement via nonlocal perception and cognitive mapping*, J. Math. Biol., 86 (2023), 71, <https://doi.org/10.1007/s00285-023-01905-9>.
- [42] Y. J. WANG, D. J. FAN, AND C. C. WANG, *Dynamics of a single population model with memory effect and spatial heterogeneity*, J. Dynam. Differential Equations, 34 (2022), pp. 1433–1452, <https://doi.org/10.1007/s10884-021-10010-8>.
- [43] Y. J. WANG, D. J. FAN, C. C. WANG, AND Y. M. CHEN, *Dynamics of a predator-prey model with memory-based diffusion*, J. Dynam. Differential Equations, (2023), <https://doi.org/10.1007/s10884-023-10305-y>.
- [44] Y. J. WANG, C. C. WANG, AND D. J. FAN, *Dynamics of a diffusive competition model with memory effect and spatial heterogeneity*, J. Math. Anal. Appl., 523 (2023), 126991, <https://doi.org/10.1016/j.jmaa.2022.126991>.

- [45] S. Y. XUE, Y. L. SONG, AND H. WANG, *Spatio-temporal dynamics in a reaction-diffusion equation with nonlocal spatial memory*, SIAM J. Appl. Dyn. Syst., 23 (2024), pp. 641–667, <https://doi.org/10.1137/22M1543860>.
- [46] H. ZHANG, H. WANG, Y. L. SONG, AND J. J. WEI, *Diffusive spatial movement with memory in an advective environment*, Nonlinearity, 36 (2023), pp. 4585–4614.
- [47] H. ZHANG, H. WANG, AND J. J. WEI, *Perceptive movement of susceptible individuals with memory*, J. Math. Biol., 86 (2023), 65, <https://doi.org/10.1007/s00285-023-01904-w>.